Half-filled stripes in a hole-doped three-orbital spin-fermion model for cuprates

Mostafa Sherif Derbala Aly Hussein, Elbio Dagotto, and Adriana Moreo

Half-filled Stripes in a Hole-Doped Three-Orbital Spin-Fermion Model for Cuprates

Mostafa Sherif Derbala Aly Hussein,[1, 2] Elbio Dagotto,[1, 2] and Adriana Moreo[1, 2]

[1]*Department of Physics and Astronomy, University of Tennessee, Knoxville, TN 37966, USA*
[2]*Materials Science and Technology Division, Oak Ridge National Laboratory, Oak Ridge, TN 37831, USA*
(Dated: February 25, 2019)

Using Monte Carlo techniques, we study a three-orbital CuO_2 spin-fermion model for copper-based high critical temperature superconductors that captures the charge-transfer properties of these compounds. Our studies reveal the presence of spin order in the parent compound and, more importantly, stripe spin and charge order under hole doping. Due to the p-d orbital hybridization, the added holes are approximately equally distributed among the two p orbitals of the oxygen atoms and the d orbital of the copper atoms in the unit cell. In rectangular clusters of dimension 16×4 *half-filled* stripes are observed upon hole doping, namely when $N_h = 2n$ holes are introduced in the system then n vertical stripes of length 4 along the short periodic direction are formed. The original antiferromagnetic order observed in the parent compound develops a $\pi-$shift across each stripe and the magnetic structure factor has a peak at wavevector $\mathbf{k} = (\pi-\delta, \pi)$ with $\delta = 2\pi N_h/N = \pi N_h/2L$, where $L = 16$. The electronic charge is also modulated and the charge structure factor is maximized at $\mathbf{k} = (2\delta, 0)$. As electrons are removed from the system, intracell orbital nematicity with $\langle n_{p_x} \rangle - \langle n_{p_y} \rangle \neq 0$ develops in the oxygen sector, as well as intercell magnetic nematicity with $\langle S^z_{\mathbf{i},d}(S^z_{\mathbf{i+x},d} - S^z_{\mathbf{i+y},d}) \rangle \neq 0$ in the spin copper sector, in the standard notation. This occurs not only in rectangular but also in square 8×8 lattices. Our results suggest that the essence of the stripe spin and charge distribution experimentally observed in hole-doped cuprates are captured by unbiased Monte Carlo studies of a simple hole-doped charge-transfer insulator CuO_2 spin-fermion model.

I. INTRODUCTION

The parent compounds of the high critical temperature (T_c) superconducting cuprates are known to be charge-transfer insulators (CTI)[1,2] with a band structure influenced by the hybridization of the $d_{x^2-y^2}$ orbital in the copper atoms and the $p_{\sigma=x,y}$ orbitals in the oxygen atoms. However, due to the technical difficulty of studying interacting many-body multiorbital Hubbard models, several of their properties, such as the incommensurate spin order and a tendency towards d-wave superconductivity upon doping, have been studied using simpler single-orbital systems, such as the one-orbital Hubbard and $t-J$ models.[2] The use of single-orbital models relies on the Zhang-Rice singlet formalism that approximately maps a three-orbital Hubbard model into an effective $t-J$ model[3] and also on the photoemission experimental observation of a single-band Fermi surface.[4–7] Despite the reasonable good agreement between numerical studies on one- and three-orbital models,[8–10] several authors have claimed that the multiorbital CuO_2 character of the cuprates plays a crucial role in their physics that cannot be neglected.[11,12] While this issue is still being debated, it is clear that models that include the p-oxygen orbitals, in addition to the d-copper orbital, are more accurate and needed to study the problem of how the doped charges are distributed. Particularly in view of the charge-transfer character of the cuprates, doped electrons primarily are located into the Cu d-orbitals, as in Mott insulators, while doped holes occupy, at least in part, the

O p-orbitals. In fact, from the Zaanen-Sawatzky-Allen (ZSA) paradigm,[1] holes doped into a CTI should reside primarily, not only partially, in the p orbitals of the oxygens. This is the assumption made in the Zhang-Rice approach[3] as well. However, recent NMR experimental results appear to indicate that the hole distribution between p and d orbitals could be material dependent.[13,14] More work is clearly needed to clarify this matter.

In addition, there is strong theoretical and experimental interest in understanding the charge structure of the stripes observed in various hole-doped cuprates.[15–20] Early experimental results in single-layer LSCO at 1/8-hole doping clearly indicated the existence of nearly static *half-filled* stripes accompanied by magnetic order commensurate with the charge stripes.[15–17] On the other hand, in bilayered YBCO, the magnetic and charge order do not appear to coexist.[18–20] On the theory front, it has been recently well-established that the stripes stabilized in the ground state of the single-orbital Hubbard model are fully filled with holes,[21] as opposed to half-filled. This appears to be a general characteristic of various single-orbital models, because it was already observed in a single-orbital spin-fermion model for the cuprates developed by some of us in the 90s[23] and, more recently, in a frustrated $t - J$ model as well.[24] Early indications of half-filled stripes observed with density matrix renormalization group (DMRG)[25] approaches in the one-orbital Hubbard models[26] are now attributed to a finite-width effect.[21,22] Nevertheless, we acknowledge that there are DMRG indications of half-filled stripes

in the $t - J$ model[27] and more recently in the Hubbard model if additional nearest-neighbor t' hoppings are added.[28,29] These extra hoppings physically originate in the O-O hopping intrinsic of multiorbital systems. In our opinion, the differences in the conclusions using different models and techniques underscores the need to move beyond single-orbital models to better investigate the ground state charge and magnetic properties of hole-doped cuprates, and to guide the construction of one-orbital models that may capture the essence of the stripes.

However, studying multiorbital models is a very challenging task. Magnetic stripes have been recently observed via Quantum Monte Carlo (QMC) simulations of a three-orbital CuO_2 Hubbard model.[30] The simulations were performed using 8×8 and 16×4 clusters, as we do below. However, due to the sign problem, the studies were carried out at high temperature ($T \approx 1,000$ K), considerably above the regime in which the charge structure of the stripes can be studied.[30] Also DMRG studies of the same model in 8×4 clusters, smaller than discussed in our publication and using external fields at the edges to stabilize the magnetic order, indicate the existence of half-filled stripes.[31] Because the above mentioned QMC results are at high temperatures without charge order and the 8×4 DMRG calculations may be affected by size effects and need external fields for magnetic stabilization, simpler alternatives to try to capture the essence of the problem are worth investigating.

For this reason, in this manuscript we study a recently introduced simple three-orbital spin-fermion model,[32] that captures the properties of the charge-transfer insulating parent compound of the cuprates and that can be studied upon doping in a wide range of temperatures and relatively large clusters. This seems ideal to explore at least qualitatively the charge and spin properties of doped cuprates. Our final goal is to find a simple model that captures the essence of the stripe formation, particularly with regards to its hole filling. A spin fermion model can be considered as an *intermediate* approach between a crude mean-field approximation, where typically results are biased towards initial assumptions made, and a detailed unbiased, but technically very hard, QMC or DMRG approach.

Our publication is organized as follows: first, the model is described in Section II; then, the magnetic and charge structures observed upon hole doping are presented in Section III; finally, Section IV is devoted to the conclusions. Overall, we believe that the simple spin-fermion CuO_2 model is able to capture the essence of the Cu-oxide physics with regards to the hole-doped system and its magnetic and charge properties. Extensions of our model to larger lattices than studied here are in principle doable using the Traveling Cluster Approximation.[33] Moreover, the model and technique allows for a study of a wide range of temperatures, from very low to very high, the addition of quenched disorder, and even the study of real-time or real-frequency dynamical and d.c.

transport properties. In these regards, we believe our effort opens a fertile area of research that will lead to qualitative progress in the study of Cu-based high-T_c superconductors and hole doped charge-transfer insulators in general.

II. MODEL

In the present effort, the three-orbital spin-fermion model for the cuprates,[32] which considers the $3d_{x^2-y^2}$ Cu and $2p_\sigma$ ($2p_x$ or $2p_y$) orbitals of the two oxygens in the CuO_2 unit cell, will be studied using primarily 8×8 and 16×4 clusters.[34] As described in our previous publication, the Hubbard repulsion at the Cu sites that splits the half-filled d-band is replaced by an effective magnetic coupling between the spin of the itinerant electrons at the d-orbital and phenomenological classical spins localized at the Cu sites. This is similar to the Mean Field Monte Carlo approximation recently introduced,[33] where the local mean-field parameters in the Hartree approximation (classical variables) are coupled to itinerant fully quantum fermions. Within this framework, an unbiased Monte Carlo simulation of the classical spins can be used to study the model. In this context, there are no sign problems which means that the whole range of doping and temperatures can be explored. Since the resulting Hamiltonian is bilinear in the fermionic operators, clusters comparable to those employed for the full multiorbital Hubbard model were studied here and using additional techniques, such as the traveling cluster approximation, substantially larger systems are potentially reachable in the future.
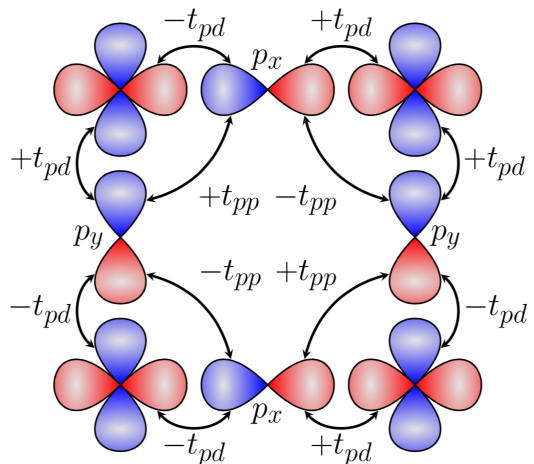

FIG. 1: (color online) Schematic drawing of the Cu $d_{x^2-y^2}$ orbitals at the copper sites of the square lattice, with the sign convention indicated by the colors (red for + and blue for -). The oxygen p_σ orbitals with their corresponding sign convention are also shown, located at the Cu-O-Cu bonds. The resulting sign convention for the t_{pd} and t_{pp} hoppings is also indicated.

More specifically, the three-orbital spin-fermion (3SF)

Hamiltonian is given by[32]

$$H_{3SF} = H_{TB} + H_{Sd} + H_{AF} + H_{Sp}, \qquad (1)$$

with

$$H_{TB} = -t_{pd} \sum_{\mathbf{i},\mu,\sigma} \alpha_{\mathbf{i},\mu}(p^\dagger_{\mathbf{i}+\frac{\hat{\mu}}{2},\mu,\sigma} d_{\mathbf{i},\sigma} + h.c.) -$$

$$t_{pp} \sum_{\mathbf{i},\langle\mu,\nu\rangle,\sigma} \alpha'_{\mathbf{i},\mu,\nu}[p^\dagger_{\mathbf{i}+\frac{\hat{\mu}}{2},\mu,\sigma}(p_{\mathbf{i}+\frac{\hat{\nu}}{2},\nu,\sigma} + p_{\mathbf{i}-\frac{\hat{\nu}}{2},\nu,\sigma}) + h.c.]$$

$$+\epsilon_d \sum_{\mathbf{i}} n^d_{\mathbf{i}} + \epsilon_p \sum_{\mathbf{i},\mu} n^p_{\mathbf{i}+\frac{\hat{\mu}}{2}} + \mu_e \sum_{\mathbf{i},\mu}(n^p_{\mathbf{i}+\frac{\hat{\mu}}{2}} + n^d_{\mathbf{i}}), \qquad (2)$$

where the operator $d^\dagger_{\mathbf{i},\sigma}$ creates an electron with spin σ at site $\mathbf{i}$ of the Cu square lattice, while $p^\dagger_{\mathbf{i}+\frac{\hat{\mu}}{2},\mu,\sigma}$ creates an electron with spin σ at orbital p_μ, where $\mu = x$ or y, for the oxygen located at $\mathbf{i} + \frac{\hat{\mu}}{2}$. The hopping amplitudes t_{pd} and t_{pp} correspond to the hybridizations between nearest-neighbors Cu-O and O-O, respectively, and $\langle\mu,\nu\rangle$ indicate O-O pairs connected by t_{pp} as indicated in Fig. 1. $n^p_{\mathbf{i}+\frac{\hat{\mu}}{2},\sigma}$ ($n^d_{\mathbf{i},\sigma}$) is the number operator for p (d) electrons with spin σ, while ϵ_d and ϵ_p are the on-site energies at the Cu and O sites, respectively. $\Delta = \epsilon_d - \epsilon_p$ is the charge-transfer gap. The signs of the Cu-O and O-O hoppings due to the symmetries of the orbitals is included in the parameters $\alpha_{\mathbf{i},\mu}$ and $\alpha'_{\mathbf{i},\mu,\nu}$ and follow the convention shown in Fig. 1. The parameter values are set to $t_{pd} = 1.3$ eV and $t_{pp} = 0.65$ eV. The on-site energy is $\epsilon_p = -3.6$ eV,[8] and thus $\Delta = \epsilon_d - \epsilon_p$ is positive since we follow the convention $\epsilon_d = 0$. The electron chemical potential is μ_e. The remaining terms of H_{3SF} are

$$H_{Sd} = J_{Sd} \sum_{\mathbf{i}} \mathbf{S}_{\mathbf{i}}.\mathbf{s}_{\mathbf{i}}, \qquad (3)$$

where $\mathbf{S}_{\mathbf{i}}$ denotes the phenomenological localized spins at site $\mathbf{i}$, while $\mathbf{s}_{\mathbf{i}} = d^\dagger_{\mathbf{i},\alpha} \vec{\sigma}_{\alpha\beta} d_{\mathbf{i},\beta}$ is the spin of the mobile d-electrons, with $\vec{\sigma}_{\alpha\beta}$ the Pauli matrices. The other two terms are:

$$H_{AF} = J_{AF} \sum_{\langle\mathbf{i},\mathbf{j}\rangle} \mathbf{S}_{\mathbf{i}}.\mathbf{S}_{\mathbf{j}}, \qquad (4)$$

and

$$H_{Sp} = J_{Sp} \sum_{\mathbf{i},\hat{\mu}} \mathbf{S}_{\mathbf{i}}.\mathbf{s}_{\mathbf{i}+\frac{\hat{\mu}}{2}}, \qquad (5)$$

where $\hat{\mu} = \pm\hat{x}$ or $\pm\hat{y}$ and $\mathbf{s}_{\mathbf{i}+\frac{\hat{\mu}}{2}} = p^\dagger_{\mathbf{i}+\frac{\hat{\mu}}{2},\mu,\alpha} \vec{\sigma}_{\alpha\beta} p_{\mathbf{i}+\frac{\hat{\mu}}{2},\mu,\beta}$.

As mentioned above, the localized spins are assumed classical[32] which allows H_{3SF} to be studied with the same Monte Carlo (MC) procedure widely employed before for the pnictides[35] and double-exchange manganites.[36] The values of the couplings, specifically $J_{AF} = 0.1$ eV, $J_{Sp} = 1$ eV, and $J_{Sd} = 3$ eV, were selected in our previous effort by comparing the orbital-resolved density of states

(DOS) with that of the three-orbital Hubbard model for cuprates obtained using the variational cluster approximation on a 12-sites cluster.[32] The calculations shown below were performed using square 8×8 and rectangular 16×4 clusters[34] with periodic boundary conditions (PBC). These sizes are comparable to those accessible at present to study the three-band Hubbard model either via quantum Monte Carlo[37–39] or via DMRG,[31] and the cluster sizes for the spin-fermion model can be increased substantially in the future. During the simulation the localized spins $\mathbf{S}_{\mathbf{i}}$ evolve using a standard Monte Carlo procedure, while the resulting single-particle fermionic matrix is exactly diagonalized. The simulations are performed at inverse temperature $\beta = (k_B T)^{-1}$ ranging from 10 to 800 in eV^{-1} units, equivalent to temperatures T from 1200 K to 15 K.[40] In the electron representation, the undoped case corresponds to one hole at the Cu's and no holes at the O's, i.e. five electrons per CuO$_2$ unit cell (the maximum possible electronic number in three orbitals is six).

III. RESULTS

A. Charge and spin structures

The undoped system with 5 electrons per unit cell shows antiferromagnetically ordered localized spins and an almost uniform distribution of the electronic charge. For $\beta = 800$ eV^{-1} ($T \sim 15$ K) we found numerically that $< n_d >= 1.164$ and $< n_{p_\sigma} >= 1.918$, close but not identical to $< n_d >= 1$ and $< n_{p_\sigma} >= 2$ which would have been the values in the absence of $p - d$ hybridization. These results are virtually independent of the cluster size used.[34] In panel (a) of Fig. 2, we display circles which are proportional to the local hole density given by $< n^h_{\mathbf{i},\alpha} >= 2- < n_{\mathbf{i},\alpha} >$ with $\alpha = d$ or p_σ and $\mathbf{i}$ the site index, using a 16×4 cluster at $T \sim 15$ K. The arrows denote the orientation of the localized spins in the $x - z$ plane and clearly show the staggered antiferromagnetic order that develops.[41] This magnetic order characterizes also the mobile quantum spins at coppers, as shown by the peak at wavevector $\mathbf{k} = (\pi, \pi)$ that develops in the magnetic structure factor in panel (a) of Fig. 3 (triangles). The uniform charge distribution is indicated by the featureless charge structure factor $N(\mathbf{k})$ shown in panel (b) of the same figure (triangles).

Consider now the case of doping corresponding to 4 holes. The charge is no longer uniformly distributed as shown in Fig. 2 (b), where in this panel the size of the circles is proportional to the difference between the density $n_{\mathbf{i},\alpha}$ and the corresponding electronic density in the undoped case, panel (a), to better visualize the stripes. It is clear from panel (b) that two hole-rich stripes develop. To a good approximation, there are two holes per stripe indicating that each stripe is *half-filled*, as it is the case in the real hole-doped cuprates according to neutron experiments.[15–20] Figure 3 (b) (crosses) shows that a distinct
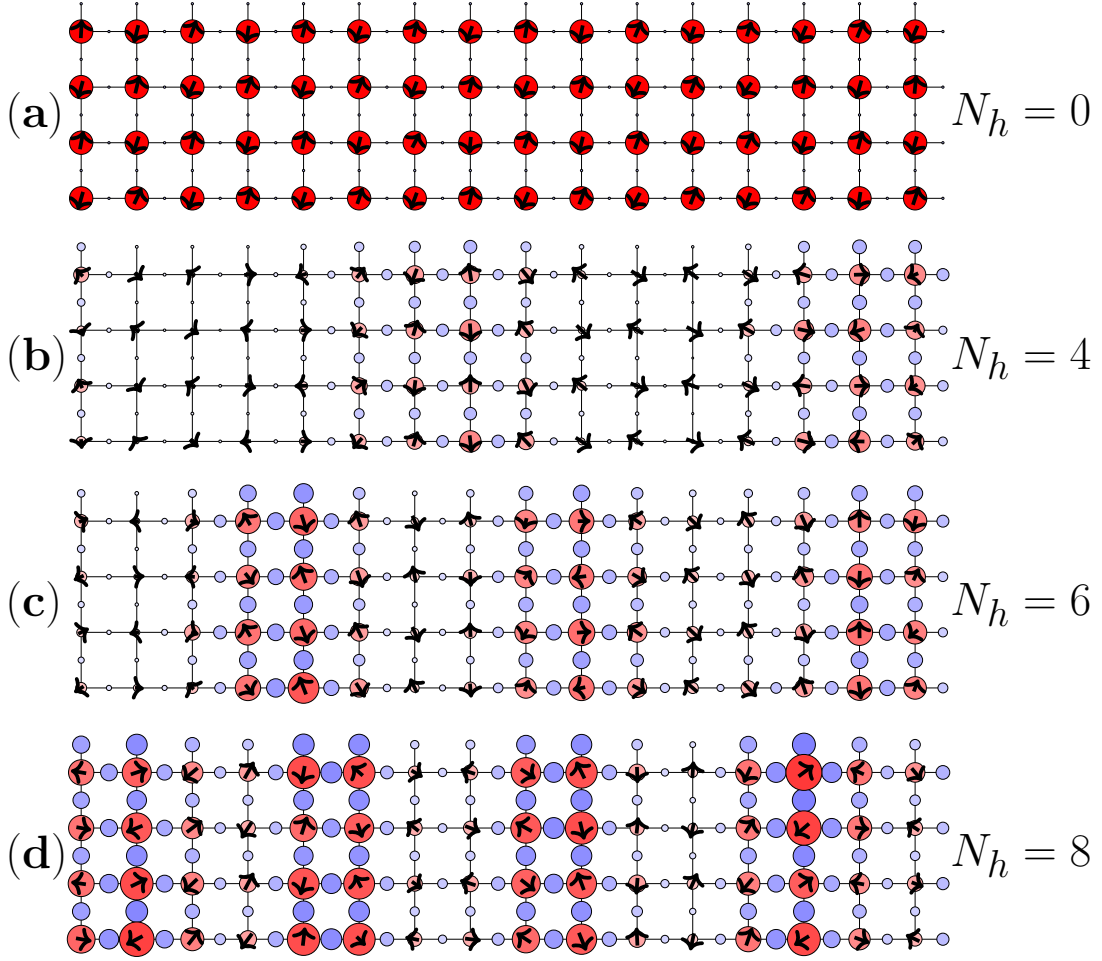
FIG. 2: (color online) Charge and spin configurations obtained with the spin-fermion model using J_{AF}=0.1 eV, J_{Sp}=1 eV, and J_{Sd}=3 eV and employing 16×4 clusters at $\beta = 800$ eV^{-1} (i.e. $T \sim 15$ K) for the following electronic densities: (a) the undoped case with 5 electrons (i.e. 1 hole) per unit cell, with the radius of the circles proportional to the hole charge which is $n_d^h = 0.82$ in the Cu sites and $n_p^h = 0.09$ in the O sites (nearly uniform distribution) for the couplings used in our Hamiltonian; (b) results for 4 doped holes; (c) 6 doped holes; (d) 8 doped holes. In panels (b), (c), and (d) the radius of the circles are proportional to the difference between the electronic density in the doped system and that in the undoped case panel (a) to better visualize the hole positions. The arrows in all panels are proportional to the classical spin projection in the $x-z$ plane shown.

feature appears in $N(\mathbf{k})$ at $\mathbf{k} = (\pi/4, 0) = (2\delta, 0)$ where δ indicates the displacement of the peak in the magnetic structure factor, that now is located at $\mathbf{k} = (\pi - \delta, \pi) = (7\pi/8, \pi)$ as shown in panel (a) of the figure (crosses). The incommensuration in the quantum spins indicates the presence of π-shifts in the magnetic order across the stripes, which can be observed also visually in the planar projection of the classical spins in Fig. 2 (b).[42]

The formation of additional half-filled stripes continues as more holes are added. For example, 6 (8) holes form 3 (4) stripes, as shown in panels (c) and (d), respectively, of Fig. 2. The evolution of the magnetic and charge incommensuration δ with doping is observed also in Fig. 3 where the peaks in the structure factors continue to shift. Notice that for 6 holes (squares) the peak in $N(\mathbf{k})$ indicates that $2\delta = 3\pi/8$, but since $k = 3\pi/16$ is not allowed in the finite lattice used, the peak in $S(\mathbf{k})$,

that should be at $(13\pi/16, \pi)$, is still located at $(7\pi/8, \pi)$ (squares). For 8 holes (circles) $\delta = \pi/4$ from the peak in $N(\mathbf{k})$ and, thus, $S(\mathbf{k})$ shows a peak at $(3\pi/4, \pi)$ which coexists with another peak at (π, π). Notice that 8 holes corresponds to 1/8 doping in the 16×4 cluster and the well-known $4a$ periodicity (with a the lattice constant) is observed. The coexistence of the incommensurate peak with that at (π, π) for 8 holes was found to be ubiquitous for this doping in our simulations. It appeared both when a random spin configuration was used as starting point of the Monte Carlo simulation or when an ordered spin configuration with a maximum at $(3\pi/4, \pi)$ in the spin structure factor was used. In both cases, ordered and disordered starting spin configurations, the simulation converged to the same final state characterized by 4 charge stripes and the double-peaked magnetic structure which we found already present in the snapshots. Larger

clusters, employing the traveling cluster approximation, will be needed in order to explore whether the peak at (π, π) arises from a finite-size effect.
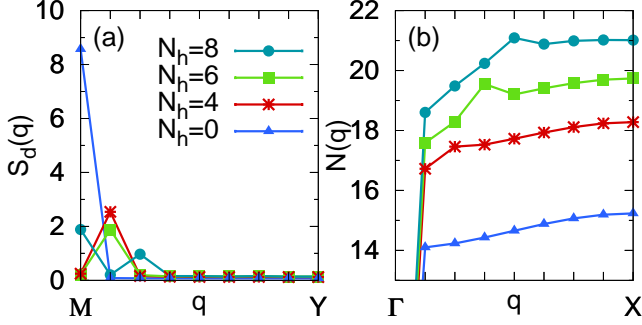

FIG. 3: (color online) (a) The magnetic structure factor $S_d(\mathbf{k})$ for the spin of the electrons in the Cu orbital along the M-Y direction in the spin-fermion model with J_{AF}=0.1 eV, J_{Sp}=1 eV, and J_{Sd}=3 eV, using a 16×4 cluster and $\beta = 800$ eV^{-1} ($T \sim 15$ K) for the number of doped holes indicated in the caption. (b) The total charge structure factor $N(\mathbf{k})$ along the Γ-X direction for the same parameters as in panel (a).

B. Nematicity

Together with the stripes, an interesting feature that develops with doping is p-orbital nematicity. In Fig. 4 (a) the orbital nematic order parameter defined as $O_n = \langle n_{\mathbf{i},p_x} - n_{\mathbf{i},p_y} \rangle$ is shown vs the number of doped holes and for values of β ranging from 10 to 800 eV^{-1} (temperatures T ranging from $\sim 1,200$ to ~ 15 K). As expected, there is no nematicity in the undoped system. However, it is clear that as hole doping increases and as the temperature decreases then nematicity develops, with a larger hole occupation of the p orbitals in the direction parallel to the stripes. It can be argued that the nematicity is merely the result of the breaking of the rotational invariance due to the shape of the 16×4 clusters used here. However, a non-neglibible nematic order parameter only develops at low temperatures and under hole doping. To further explore this issue we evaluated the nematicity in a *symmetric* 8×8 cluster. Here, no nematicity was observed in O_n, panel (b), but this could be due to the coexistence of nematic regions with positive and negative values of O_n switching from one another during the Monte Carlo time evolution, or simply a coherent quantum mechanical superposition of both orientations.

To explore this possibility we studied the modified order parameter $|O|_n = \langle |n_{\mathbf{i},p_x} - n_{\mathbf{i},p_y}| \rangle$. This order parameter does *not* change sign if the orientation of the stripes switches from vertical to horizontal. While at high temperatures it is natural that thermal fluctuations locally establish a difference between the two directions from site to site, thus rendering $|O|_n$ nonzero even for zero holes, as the temperature is lowered thermal fluctuations are reduced and the order parameter $|O|_n$ becomes zero in the undoped limit because there are no stripes at tem-
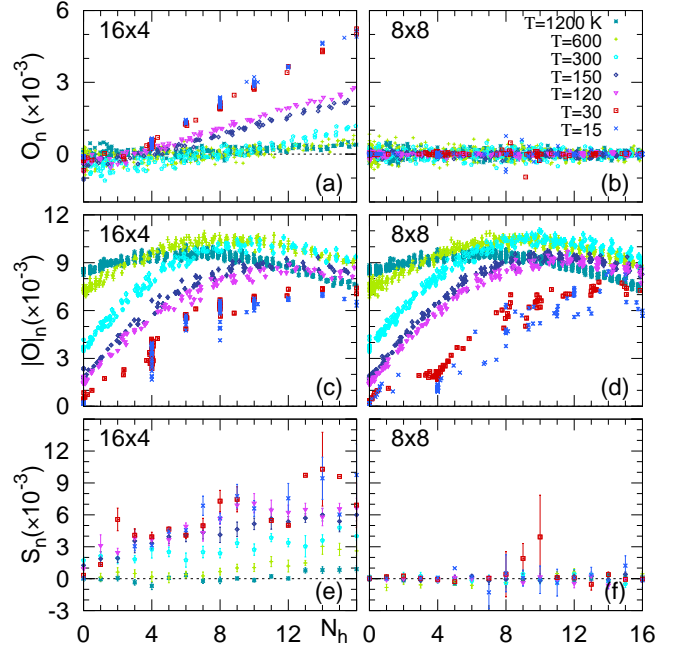

FIG. 4: (color online) Orbital nematic order parameter $O_n = \langle n_{\mathbf{i},p_x} - n_{\mathbf{i},p_y} \rangle$ varying the doped number of holes at the βs indicated in the inset, employing a spin-fermion model with J_{AF}=0.1 eV, J_{Sp}=1 eV, and J_{Sd}=3 eV. In panel (a) a 16×4 cluster is used. Panel (b) is the same as (a) but employing an 8×8 cluster. In (c) the nematicity is given by $|O|_n = \langle |n_{\mathbf{i},p_x} - n_{\mathbf{i},p_y}| \rangle$ using a 16×4 cluster with the same parameters as panel (a). Panel (d) is the same as (c) but in an 8×8 cluster. Panel (e) same as (a) but for the spin nematic order parameter $S_n = \langle S^z_{\mathbf{i},d}(S^z_{\mathbf{i}+\mathbf{x},d} - S^z_{\mathbf{i}+\mathbf{y},d}) \rangle$. Panel (f) is the same as (e) but using an 8×8 cluster.

peratures sufficiently low. However, the results for the doped system are qualitatively different.

In panel (c) of Fig. 4 $|O|_n$ is ploted vs hole doping and at various temperatures for the 16×4 cluster. As expected its value decreases with temperature and at $\beta = 400$ and 800 eV^{-1} (temperatures $T \sim 30$ and ~ 15 K, respectively) the data for O_n in panel (a) are qualitatively reproduced (although with different slopes). The Monte Carlo results for $|O|_n$ in the 8×8 cluster are shown in panel (d) of the figure. It is remarkable to observe that the curves are very *similar* to those for the 16×4 cluster in panel (c). In fact, in the undoped case it is clear that the order parameter $|O|_n$ for the square lattice converges to zero, as expected, at low temperatures where the thermal fluctuations are small, while it remains nonzero at finite doping even at the lowest temperatures investigated. This clearly supports the notion that the absence of stripes on the 8×8 cluster is due to a cancellation between both orientations, with each one dominating in different regions of the system. Local nematicity for the square lattice with periodic boundary conditions in both directions is present even at the lowest temperatures reached in our numerical simulations, but combined with the results shown in panel (b) we can deduce that in about 50% of the sites $n_{\mathbf{i},p_x} > n_{\mathbf{i},p_y}$ and

vice versa. Namely, there is an asymmetry between the x and y directions. Again, it is also clear that there is no nematicity in the undoped system at low temperature, even using rectangular clusters that in principle break explicitly the lattice rotational invariance. However, the nematicity clearly increases with hole doping.

Scanning tunneling microscopy (STM) experiments have reported intracell nematicity in the p orbitals in underdoped $Bi_2Sr_2CaCu_2O_{8+\delta}$ (Bi-2212)[43] and in the overdoped regime of $(Bi,Pb)_2Sr_2CuO_{6+\delta}$ (Bi-2201).[44] The nematicity found was attributed to inequivalence in the electronic structure at the two oxygen sites within each unit cell, but the experiments could not disentangle whether it was of charge or magnetic origin. Our results indicate that the nematicity arises from a charge difference among the intracell p_σ orbitals.

In addition, the previously mentioned STM experiments[43,44] did not observe nematicity associated with the d orbitals. However, the results of Resonant X-ray Scattering in the stripe phase of $(La,M)_2CuO_4$ (M=Sr, Ba, Eu, or Nd)[45] reported nematicity in the d orbitals. Our simulations indicate that the spin correlations among the spin of the electrons in the p orbitals are much smaller than those among the d electrons and no magnetic nematicity in the p orbitals was observed. However, we studied the charge correlations along the x and y direction for the d orbital and its corresponding spin-nematic order parameter $S_n = \langle S^z_{\mathbf{i},d}(S^z_{\mathbf{i+x},d} - S^z_{\mathbf{i+y},d})\rangle$. While no nematicity was observed in the charge correlations we found that in the 16×4 cluster the nearest-neighbor antiferromagnetic correlations are stronger (weaker) in the direction parallel (perpendicular) to the stripes and the anisotropy increases when the temperature decreases, as shown in Fig. 4 (e). The corresponding results in the 8×8 cluster, panel (f), do not display nematicity, but we believe that, as in the orbital case, panel (b), this is merely due to the equal presence of coexisting regions with both orientations of the nematicity. After all, if the charge patterns are an equal-weight mixture of vertical and horizontal stripes, the same has to occur for the spin textures.

We have also studied how the orbital nematicity and the magnetic and charge incommensurability develop vs temperature and doping. In the left column of Fig. 5 the orbital nematic order parameter O_n, panel (a), the magnetic structure factor as its maximum value $\mathbf{k}_{max} = (7\pi/8, \pi)$, panel (d), and the charge structure factor as its maximum value $\mathbf{k}_{max} = (3\pi/4, 0)$ relative to its value at $\mathbf{k} = (\pi/8, 0)$, panel (g), are presented for the case of 4 doped holes in the 16×4 cluster. The three order parameters start developing at approximately the same temperature between 200 K and 300 K. For 6 doped holes the corresponding results appear in panels (b), (e), and (h) of the same figure and it can be observed that the three magnitudes start to increase at temperatures below $T \approx 300$ K. Finally, in panels (c), (f), and (i) the results for $N_h = 8$ are presented. Now the temperature below which the three order parameters start rising is lower

with $T \approx 200$ K.

These results seem to indicate that magnetic and charge incommensurability develop simultaneously with the nematicity. Thus, no purely isolated nematic phase is observed upon cooling. The presence of magnetic stripes at high temperature as reported in quantum Monte Carlo simulations of a three-band Hubbard model[30] is not detected by our approach either. We indeed used the approach in Ref.[30] to understand how the cluster geometry affects the formation of stripes. We measured the quantum spin-spin correlations for the d electrons $S^z(\ell, d) = \langle S^z_{\mathbf{i},d}S^z_{\mathbf{i}+\ell,d}\rangle$. in real space and in panel (a) of Fig. 6 we display $(-1)^{|\ell_x+\ell_y|}S^z(\ell, d)$ in an 8×8 cluster at $\beta = 800$ eV^{-1} ($T \sim 15$ K) doped with 8 holes. A structure consistent with coexisting vertical and horizontal half-filled stripes as in Ref.[30] is observed: near the origin of coordinates bottom left, the blue tone points indicate a standard staggered spin pattern, while the red tone points elsewhere indicate the presence of a π-shift in the staggered pattern as it occurs in the presence of stripes. It is remarkable that a similar pattern is obtained in both the three-band Hubbard model and in the three-band spin fermion model using different numerical methods. However, we have only identified these structures at low temperatures, corresponding to the temperatures for which the stripes are well developed in the 16×4 clusters. In addition, in Fig. 6 (b) it can be seen that the charge distribution is also consistent with the coexistence of one horizontal and one vertical half-filled stripe.

C. Total vs orbital doping

Finally, we want to address the issue of whether the properties of the cuprates should be discussed in terms of the total doping or instead focusing on the local n_d and n_p doping as proposed in Refs..[13,14] NMR measurements in different superconducting cuprates indicate that the change in the electronic density in the d and p orbitals as holes are added to the system is material dependent. In the undoped case, with one hole per unit cell, the hole would be expected to be located at the Cu's so that the density of holes in the d orbitals $\langle n^h_d \rangle = 1$ while the density of holes in the p orbitals would be $\langle n^h_{p_x} \rangle = \langle n^h_{p_y} \rangle = 0$. However, experiments indicate that while the relationship $\langle n^h_d \rangle + \langle n^h_{p_x} \rangle + \langle n^h_{p_y} \rangle = 1$ is satisfied, the holes are distributed among the three orbitals in an hybridization dependent way peculiar to each material with $\langle n_d \rangle$ ranging from 0.82 for the case of La-214 (circles in Fig. 7) to about 0.68 for Y-123 (squares in Fig. 7), and finally to about 0.5 for Tl-2223 (green symbols in Fig. 7).[13,14]

The results for $\langle n^h_d \rangle$ versus $\langle n^h_{p_x} \rangle + \langle n^h_{p_y} \rangle$ meassured in the spin-fermion model with the usual set of parameters are also plotted in Fig. 7 for various values of the inverse temperature β and in 16×4 and 8×8 clusters. Our results indicate that the orbital distribution of holes has a weak temperature dependence. We observed that the hole distribution between d and p electrons repro-
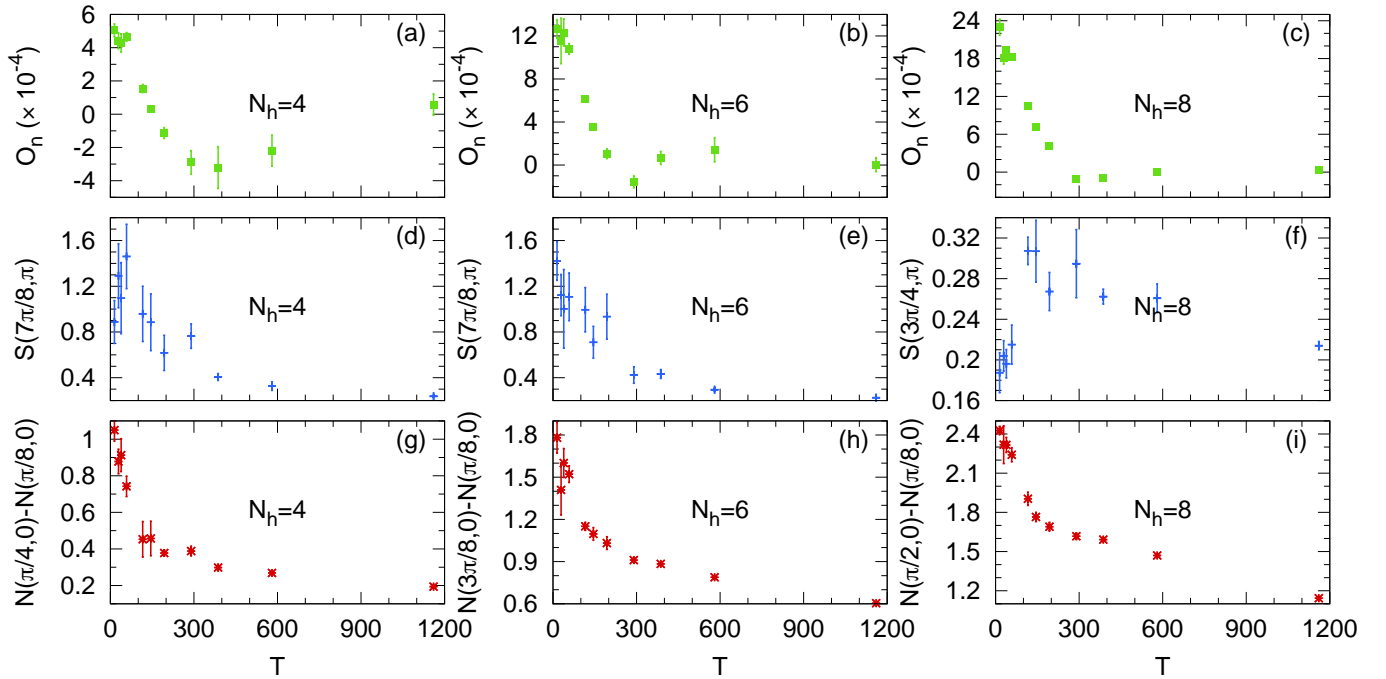
FIG. 5: (color online) Orbital nematic order parameter $O_n = \langle n_{\mathbf{i},p_x} - n_{\mathbf{i},p_y} \rangle$ vs temperature T for (a) 4 holes $N_h = 4$, (b) 6 holes $N_h = 6$, and (c) 8 holes $N_h = 8$. Also shown is the magnetic structure factor $S(\mathbf{k}_{max})$ at the wavevector where it is maximized vs temperature for (d) $N_h = 4$ and $\mathbf{k}_{max} = (7\pi/8, \pi)$, (e) $N_h = 6$ and $\mathbf{k}_{max} = (7\pi/8, \pi)$, and (f) $N_h = 8$ and $\mathbf{k}_{max} = (3\pi/4, \pi)$. Similarly, we present an analogous analysis for the charge. Shown are the maximum value of the charge structure factor $N(\mathbf{k}_{max}) - N(\pi/8, 0)$ vs temperature for (g) $N_h = 4$ and $\mathbf{k}_{max} = (\pi/4, 0)$, (h) $N_h = 6$ and $\mathbf{k}_{max} = (3\pi/8, 0)$, and (i) $N_h = 8$ and $\mathbf{k}_{max} = (\pi/2, 0)$. The results are for the spin-fermion model with J_{AF}=0.1 eV, J_{Sp}=1 eV, and J_{Sd}=3 eV using a 16×4 cluster.

duces the experimental results for La-214 in the undoped case. Experimentally it was also observed that the rate at which doped holes distribute among the d and p orbitals is material dependent and it is given by the slope of the curves shown in the figure. The slope that we observed is larger than the one obtained experimentally for the Hg and Tl compounds which, as shown in the figure, is slightly higher than the results for La-214.[13,14] The parameters used in our calculations where obtained from comparisons with ARPES results obtained mostly in BISCO compounds[32] for which experimental results for $\langle n_d^h \rangle$ versus $\langle n_{p_x}^h \rangle + \langle n_{p_y}^h \rangle$ are not available. In this respect, the excellent agreement with LSCO results may be accidental. We believe that a fine tuning of the parameters of the model, particularly in the tight-binding term, may improve quantitatively the agreement for all materials. However, it is important to notice that *qualitatively* the material dependent distribution of the doped holes among the different orbitals in the unit cell is indeed captured by the spin-fermion model. This result indicates that some properties of the cuprates may be more dependent on the way in which the holes are distributed among the Cu and O orbitals than on the total density of doped holes.

IV. CONCLUSIONS

In this publication, we present the results of Monte Carlo studies of a phenomenological three-orbital CuO_2 spin-fermion model that captures the charge-transfer properties of the superconducting cuprates. The differences between a Mott and a charge transfer insulator are relevant upon hole doping, the regime of main focus in our present study. One of the most peculiar properties of hole-doped cuprates is the formation of hole half-filled stripes (one hole every two sites along the stripe),[15–20,46–49] as opposed to hole fully-filled stripes. This is a behavior that is not reproduced in the single-orbital Hubbard model[21,22] and it has only been observed in three-orbital Hubbard models using DMRG techniques in small clusters because of the numerical challenge represented by this formidable problem. Moreover, the Quantum Monte Carlo studies of three-band Hubbard models can only be performed at temperatures above 1000 K, due to sign problems, where charge stripes do not exist. Thus, it is important to find simpler alternatives that capture the qualitative essence of the problem without such computational complexity.

The present calculation obtains for the first time *half-filled charge stripes* with unbiased numerical calculations of a simple spin-fermion three-orbital charge-transfer system. In general, it is difficult to study the stripes in
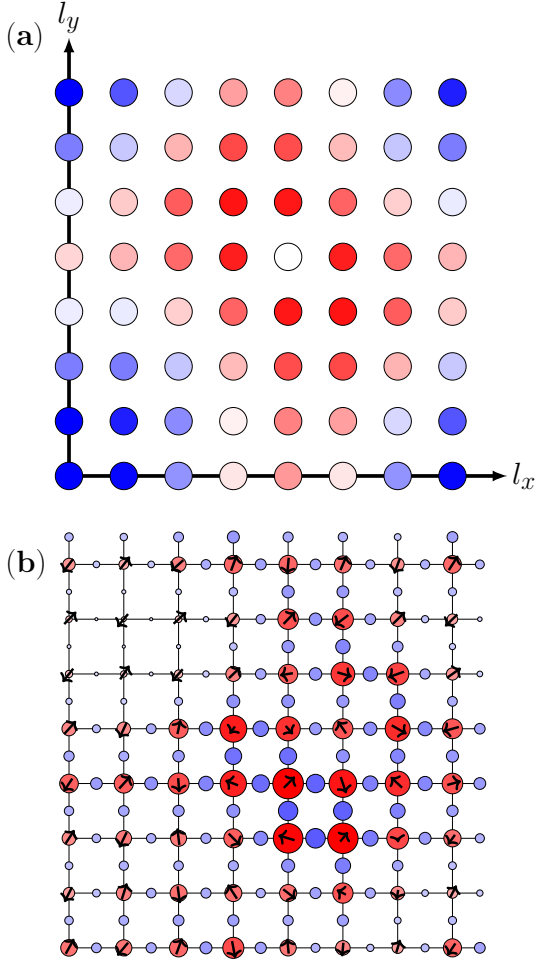
FIG. 6: (color online) (a) Real-space spin correlation functions $(-1)^{|\ell_x+\ell_y|}S^z(\ell,d)$ for the electrons in the d orbital using an 8×8 cluster with 8 doped holes at $\beta = 800$ eV^{-1} ($T \sim 15$ K) and employing the spin-fermion model with $J_{\rm AF}$=0.1 eV, $J_{\rm Sp}$=1 eV, and $J_{\rm Sd}$=3 eV. The blue tone points near (0,0) bottom left, indicate a standard spin antiferromagnetic pattern. The red tone points indicate a spin correlation that has changed sign, namely the presence of a π-shift as it occurs in the presence of stripes. (b) Snapshot of the final configuration in a Monte Carlo run for the parameters in (a) showing the charge distribution and the classical spins projection in the $x-z$ plane, as in Fig. 2.
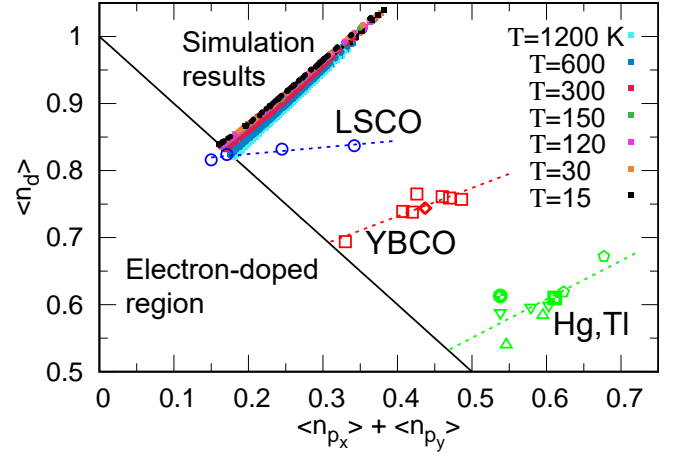

FIG. 7: (color online) Density of holes in the d orbital vs the total hole density in the p orbitals for the spin-fermion model with $J_{\rm AF}$=0.1 eV, $J_{\rm Sp}$=1 eV, and $J_{\rm Sd}$=3 eV using 16×4 and 8×8 clusters for the temperatures indicated in the caption and for different hole densities, ranging from 0 holes (left) to 20 holes (right). The solid line indicates $\langle n_d \rangle + \langle n_{p_x} \rangle + \langle n_{p_y} \rangle = 1$ satisfied by the undoped system. Experimental results for hole doped La-214 (LSCO) (circles), Y-124 (diamonds) and Y-123 (squares) (YBCO), and Hg- and Tl-based cuprates (green symbols) (Hg-1201, Tl-2212, Tl-2223, Tl-2201) were kindly provided by the authors of Ref..[13] For reference, $\beta = 800$ eV^{-1} means $T \sim 15$ K, while $\beta = 10$ eV^{-1} means $T \sim 1,200$ K.

square clusters because during the Monte Carlo time evolution both vertical and horizontal stripes develop and the results represent *averages* in both directions. However, in rectangular 16×4 clusters the development of half-filled stripes, accompanied by magnetic π-shifts across the stripes is clear and properly captures the experimental results in the cuprates. In addition, we observed orbital nematicity, due to an asymmetry in the charge distribution between the p_x and p_y orbitals in agreement with results from STM experiments.[43,44] Focusing on the copper d-orbital the nematicity observed with Resonant X-ray Scattering in the striped phase of $({\rm La,M})_2{\rm CuO}_4$[45] was also found in our analysis.

Using 8×8 clusters, and by focusing on the absolute value of the nematic order parameter, we unveiled tendencies towards half-filled stripes even in square clusters: the average over long runs appears featureless but by using absolute values it can be shown that there is nematicity even in square clusters. One relatively minor problem in our study is that we found difficult to address the issue of whether the stripes are centered at the d or the p orbitals because the excess holes do not form sharp domains, as can be seen in Fig. 2, but instead they have a finite width.

These results also demonstrate the crucial role that the hybridization between the d copper orbitals and the p oxygen orbitals play in the formation of half-filled stripes. In fact, in the limit in which the oxygen bands in the current model are pushed far away from the Fermi surface, the model becomes equivalent to the single-orbital spin-fermion model,[23] which was studied before and has filled stripes. Our work also provides justification to the need to add a phenomenological plaquette diagonal hopping to the single-orbital Hubbard model in order to transition from filled to the half-filled stripes recently reported[28,29]: the t' hopping captures the "bridge" effect to allow diagonal electronic movement among the d orbitals provided by the p orbitals at the oxygens.

The correct magnetic properties are also captured by the spin-fermion model that displays clear tendencies towards long-range antiferromagnetic order in the undoped case, and it also starts to develop incipient indications of incommensurability along $(\pi-\delta,\pi)$ and $(\pi,\pi-\delta)$ in

the doped case. The coexistance of charge and magnetic order is material dependent in the cuprates and, in the present model, it is possible that these properties could be captured by modifications of the parameters in the present model. In addition, these particular features that develop upon hole doping, likely originate in stripes, although they could also result from intertwinned orders, and they appear to require rectangular clusters for their proper stabilization. Future work will address even larger lattices (employing techniques developed for spin-fermion-like models in contexts such as manganites), a detailed temperature dependence, and the influence of quenched disorder on the appearance of stripes in CuO_2 spin-fermion models.

V. ACKNOWLEDGMENTS

[1] J. G. Zaanen, G. A. Sawatzky, and J. W. Allen, Phys. Rev. Lett. **55**, 418 (1985).

[2] E. Dagotto, Rev. Mod. Phys. **66**, 763 (1994) and references therein.

[3] F. C. Zhang and T. M. Rice, Phys. Rev. B **37**, 3759 (1988).

[4] Z.-X. Shen, J. W. Allen, J. J. Yeh, J. -S. Kang, W. Ellis, W. Spicer, I. Lindau, M. B. Maple, Y. D. Dalichaouch, M. S. Torikachvili, J. Z. Sun, and T. H. Geballe, Phys. Rev. B **36**, 8414 (1987).

[5] J. W. Allen, C. G. Olson, M. B. Maple, J.-S. Kang, L. Z. Liu, J.-H. Park, R. O. Anderson, W. P. Ellis, J. T. Markert, Y. Dalichaouch, and R. Liu, Phys. Rev. Lett **64**, 595 (1990).

[6] B. O. Wells, Z-X. Shen, A. Matsuura, D. M. King, M. A. Kastner, M. Greven, and R. J. Birgeneau, Phys. Rev. Lett **74**, 964 (1995).

[7] A. Damascelli, Z. Hussain, and Z.-X. Shen, Rev. Mod. Phys. **75**, 473 (2003).

[8] M. S. Hybertsen, M. Schlütter, and N. E. Christensen, Phys. Rev. B **39**, 9028 (1989).

[9] Silvia B. Bacci, Eduardo R. Gagliano, Richard M. Martin, and James F. Annett, Phys. Rev. B **44**, 7504 (1991).

[10] E. Arrigoni, M. Aichhorn, M. Daghofer, and W. Hanke, New J. Phys. **11**, 055066 (2009).

[11] V. J. Emery, Phys. Rev. Lett. **58**, 2794 (1987).

[12] Bayo Lau, Moma Berciu, and George A. Sawatzky, Phys. Rev. Lett. **106**, 036401 (2011).

[13] M. Jurkutat, D. Rybicki, O. P. Sushkov, G.V.M. Williams, A. Erb, and J. Haase, Phys. Rev. B **90**, 140504(R) (2014).

[14] D. Rybicki, M. Jurkutat, S. Reichardt, C. Kapusta, and J. Haase, Nat. Comm. **7**, 11413 (2016).

[15] J. M. Tranquada, B. Sternlieb, J. Axe, Y. Nakamura, and S. Uchida, Nature **375**, 561 (1995).

[16] R. J. Birgeneau, C. Stock, J. M. Tranquada, and K. Yamada, J. Phys. Soc. Jpn, **75** 111003 (2006).

[17] J. M. Tranquada, Physica B **407**, 1771 (2012).

[18] S. Blanco-Canosa, A. Frano, T. Loew, Y. Lu, J. Porras, G. Ghiringhelli, M. Minola, C. Mazzoli, L. Braicovich, E. Schierle, E. Weschke, M. Le Tacon, and B. Keimer, Phys. Rev. Lett. **110**, 187001 (2013).

[19] M. Hücker, N. B. Christensen, A. T. Holmes, E. Blackburn, E. M. Forgan, R. Liang, D. A. Bonn, W. N. Hardy, O. Gutowski, M. v. Zimmermann, S. M. Hayden, and J. Chang, Phys. Rev. B **90**, 054514 (2014).

[20] S. Blanco-Canosa, A. Frano, E. Schierle, J. Porras, T. Loew, M. Minola, M. Bluschke, E. Weschke, B. Keimer, and M. Le Tacon, Phys. Rev. B **90**, 054513 (2014).

[21] B-X. Zheng, C-M. Chung, P. Corboz, G. Ehlers, M-P. Qin, R. M. Noack, H. Shi, S. R. White, S. Zhang, G. K-L. Chan, Science **358**, 1155 (2017).

[22] G. Ehlers, S. R. White, and R. M. Noack, Phys. Rev. B **95**, 125125 (2017).

[23] C. Buhler, S. Yunoki, and A. Moreo, Phys. Rev. Lett. **84**, 2690 (2000).

[24] J. F. Dodaro, H-C. Jiang, and S. A. Kivelson, Phys. Rev. B **95**, 155116 (2017).

[25] S. R. White, Phys. Rev. Lett. **69**, 2863 (1992); Phys. Rev. B **48**, 10345 (1993).

[26] S. R. White and D. J. Scalapino, Phys. Rev. Lett. **91**, 136403 (2003).

[27] S. R. White and D. J. Scalapino, Phys. Rev. Lett. **80**, 1272 (1998).

[28] E. W. Huang, C. B. Mendl, H. C. Jiang, B. Moritz, and T. P. Devereaux, NPJ Quantum Materials **3** (2018).

[29] H-C. Jiang and T. P. Devereaux, arXiv:1806.01465.

[30] E. W. Huang, C. B. Mendl, S. Liu, S. Johnston, H-C. Jiang, B. Moritz, and T. P. Devereaux, Science **358**, 1161 (2017).

[31] S. R. White and D. J. Scalapino, Phys. Rev. B **92**, 205112 (2015).

[32] Mostafa Sherif Derbala Aly Hussein, Maria Daghofer, Elbio Dagotto, and Adriana Moreo, Phys. Rev. B **98**, 035124 (2018).

[33] A. Mukherjee, N. D. Patel, S. Dong, S. Johnston, A. Moreo, and E. Dagotto, Phys. Rev. B **90**, 205133 (2014); A. Mukherjee, N. D. Patel, C. Bishop, and E. Dagotto, Phys. Rev. E **91**, 063303 (2015).

[34] Some runs in 12×6 and 12×8 clusters were also performed, corroborating the results obtained in the smaller clusters.

[35] Shuhua Liang, Adriana Moreo, and Elbio Dagotto, Phys. Rev. Lett. **111**, 047004 (2013). See also Shuhua Liang, Gonzalo Alvarez, Cengiz Sen, Adriana Moreo, and Elbio Dagotto, Phys. Rev. Lett. **109**, 047001 (2012).

[36] E. Dagotto, S. Yunoki, A. L. Malvezzi, A. Moreo, J. Hu, S. Capponi, D. Poilblanc, and N. Furukawa, Phys. Rev. B **58**, 6414 (1998).

[37] G. Dopf, A. Muramatsu, and W. Hanke, Phys. Rev. B **41**, 9264 (1990).

[38] Z. B. Huang, H. Q. Lin and J. E. Gubernatis, Phys. Rev. B **63**, 115112 (2001).

[39] Y. F. Kung, C.-C. Chen, Y. Wang, E. W. Huang, E. A. Nowadnick, B. Moritz, R. T. Scalettar, S. Johnston, and T. P. Devereaux, Phys. Rev. B **93**, 155166 (2016).

[40] The temperature T in Kelvin degrees is obtained using $T = 11,605/\beta$.

[41] The spins of the electrons in the d orbital are oriented antiparallel to the classical spins.

[42] The π-shift in the classical spins manifests itself as a slow rotation.

[43] M. J. Lawler, K. Fujita, J. Lee, A. R. Schmidt, Y. Kohsaka, C. K. Kim, H. Eisaki, S. Uchida, J. C. Davis, J. P. Sethna, and E-A. Kim, Nature **466** 347 (2010).

[44] Y. Zheng, Y. Fei, K. Bu, W. Zhang, Y. Ding, X. Zhou, J. E. Hoffman, and Y. Yin, Scientific Reports **7**, 8059 (2017).

[45] A. J. Achkar, M. Zwiebler, Christopher McMahon1, F. He, R. Sutarto, Isaiah Djianto, Zhihao Hao, Michel J. P. Gingras, M. Hücker, G. D. Gu, A. Revcolevschi, H. Zhang, Y.-J. Kim, J. Geck, D. G. Hawthorn, Science **351** 576 (2016).

[46] S. W. Cheong, G. Aeppli, T. E. Mason, H. Mook, S. M. Hayden, P. C. Canfield, Z. Fisk, K. N. Clausen, and J. L. Martinez, Phys. Rev. Lett **67**, 1791 (1991).

[47] J. M. Tranquada, J. D. Axe, N. Ichikawa, A. R. Moodenbaugh, Y. Nakamura, and S. Uchida, Phys. Rev. Lett. **78**, 338 (1997).

[48] P. Dai, H. A. Mook, and F. Dogan, Phys. Rev. Lett **80**, 1738 (1998).

[49] H. A. Mook, P. Dai, S. M. Hayden, G. Aeppli, T. G. Perring, and F. Dogan, Nature (London) **395**, 580 (1998).